RSC Advances

ROYAL SOCIETY OF CHEMISTRY

www.rsc.org/advances

Graphical Abstract

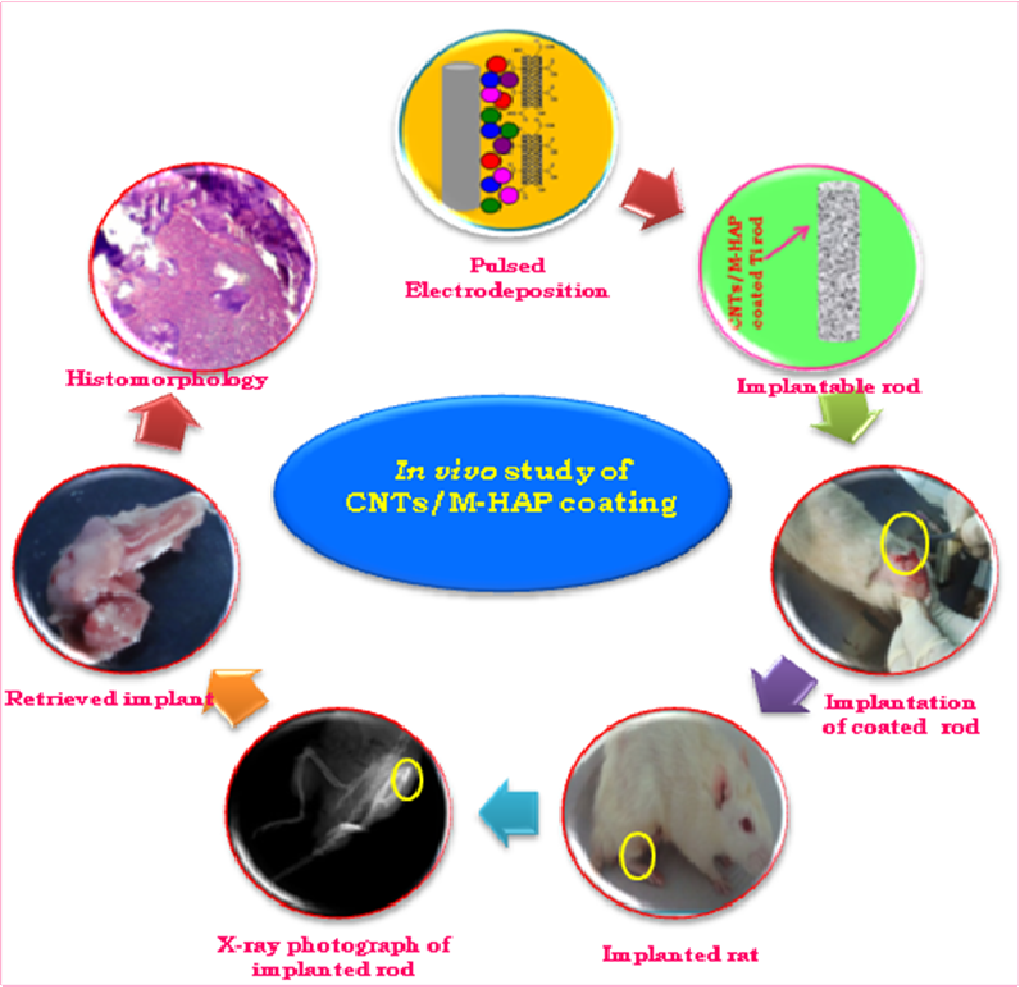

Single walled carbon nanotubes reinforced mineralized hydroxyapatite composite coatings on titanium for improved biocompatible implant applications

D. Gopi[a,b,*], E. Shinyjoy[a], A. Karthika[a], S. Nithiya[a], D. Rajeswari[a] , L. Kavitha[c] and Tingting Tang[d]

[a] *Department of Chemistry, Periyar University, Salem 636011, Tamilnadu, India*

[b] *Centre for Nanoscience and Nanotechnology, Periyar University, Salem 636011,Tamilnadu, India*

[c] *Department of Physics, School of Basic and Applied Sciences, Central University of Tamilnadu, Thiruvarur 610 101, Tamilnadu, India*

[d] *Department of Orthopedic Surgery, Shanghai Ninth People's Hospital, Shanghai Jiaotong University School of Medicine, 639 Zhizaoju Road, Shanghai 20011, P.R. of China*

*Corresponding author. Tel.: +91 427 2345766; fax: +91 427 2345124.

E-mail address: dhanaraj_gopi@yahoo.com (D. Gopi)

ABSTRACT

A surface coating strategy encompassing the use of bioactive trace elements and reinforcing material will have a significant influence on the mechanical and osseointegration properties of bioceramic coated implants. Here, we developed minerals substituted hydroxyapatite (M-HAP) and carbon nanotubes reinforced mineralized hydroxyapatite (CNT/M-HAP) composite coating on titanium (Ti) by pulsed electrodeposition which is a promising approach to produce bioimplants with better osseointegration capacity and improved mechanical property. The role of CNT and minerals like strontium, magnesium and zinc, in enhancing the mechanical and biological properties of HAP coating was investigated using various techniques. The structural and morphological analyses were carried out using Fourier transform infrared spectroscopy, X-ray diffraction analysis, scanning electron microscopy, energy dispersive X-ray analysis and elemental mapping. The mechanical characterization results revealed enhanced adhesion strength for the composite coating. Also, an improved viability of osteoblast cells was

observed *in vitro* on the CNT/M-HAP composite coating. The ability of the composite coated Ti implant to induce bone formation was evaluated *in vivo* in Wistar rats. Thus, the as-developed composite coated Ti that combines the good osteoconductivity of M-HAP together with the mechanical strength of CNT can be used as a potential implant material for orthopedic applications.

Keywords: Single walled CNT, Biocompatibility, Cell viability, Mineralized HAP, *In vivo* test, Osseointegration.

1. Introduction

The repair and replacement of injured or malfunctioning bone has become a critical problem in orthopaedic and dental surgery. In recent years, a noteworthy development has been made in the area of organ replacement and the use of artificial or synthetic prostheses in treating the loss or failure of an organ.[1] Implantation of synthetic graft by using metals, ceramics and polymers is the preferred method for the reconstruction and repair of bone lesions.[2] But the available bio-ceramics and biocompatible metals do not fulfill the requirements. The ceramics has low fracture toughness than human cortical bone and no metal has the ability to directly bond with living bone.[3] However, the artificial implants made of metals or alloys like Ti, stainless steel, cobalt-chromium, magnesium and nickel based alloys are utilized for bone replacements. The implant material used for high load bearing bones such as femoral and tibia bones should possess bone bonding ability and high fracture toughness.[4,5] To satisfy the need, the metallic implants preferably made of Ti is generally used in orthopedic applications.[6,7] Though Ti implant is successful in dental and orthopedic applications, effort has gone in improving the implant-tissue osseointegration. Among the various attempts made to improve the osseointegration process, the bioactive material like hydroxyapatite [$(Ca_{10}(PO_4)_6(OH)_2$, HAP] has received more attention in orthopedic surgery as a bone replacing material due to its bioactivity,

biocompatibility and excellent adaptation under *in vivo* conditions.[8-10] The improved biocompatibility of HAP coatings is due to the chemical and biological similarity of HAP to hard tissues, and its consequent direct bonding to host bones.[11] HAP which is naturally occurring in bone is a multi-substituted calcium phosphate that includes traces of Mg^{2+}, F^{-}, CO_3^{2-}, Sr^{2+}, Si^{4+}, Zn^{2+}, Ce^{2+}, Li^{+} etc.[12-14] The biocompatibility and bioactive property of HAP can be tailored over a wide range by modifying the composition via ionic substitutions. These ionic substitutions are considered to play an important role for the formation of bone. Thus, the substitution of bioactive minerals in HAP ensures the long term clinical application and enhances the bioactivity of HAP coatings and thereby, helps in promoting the osseointegration process.[15,16]

The incorporation of specific elements can then be used to tune the biological properties of apatite. Concerning the biological properties of the composite coatings we have tried for the combination of bioactive elements such as strontium (Sr), magnesium (Mg), and zinc (Zn) into the HAP coatings to induce favorable biological effects. Among the various minerals used in the substitution for HAP, Sr is one of the most abundant and nutritionally essential trace elements present in the human body. Sr promotes bone formation and thereby favors bone healing by enhancing the osteoblast proliferation. A preceding study confirmed that the effects of calcium and strontium on metabolic behavior are almost identical in the skeletal system. In both *in vitro* and *in vivo* tests, Sr promotes osteoblast proliferation and inhibits osteoclast proliferation, and *in vitro* animal experiments have shown that strontium enhances the bone regeneration.[17-20]

Magnesium is the fourth most abundant cation in living organisms. Mg acts as a cofactor for many enzymatic reactions, some of which are known to induce the proliferation of osteoblast cells.[21,22] They directly affect the process of mineralization and mechanical properties of bones. The Mg ions incorporated FG$MgCO_3$Ap-collagen composite exhibited osteoblast adhesion to apatite and promoted bone formation which is clearly evidenced from their *in vitro* and *in vivo*

studies.[23] Therefore, it is logical to incorporate Mg ions into HAP coating simultaneously to improve both the bioactivity and long term stability of the coating. Mg deficiency affects all skeletal metabolism stages causing decrease in osteoblastic and osteoclastic activities, cessation of bone growth and generation of osteopenia and bone fragility. Mg, therefore, plays an active role on "new bone tissue generation" process.[24,25]

Similarly, zinc substitution in HAP has been the focus of particular interest because of its diverse roles in biological functions. It is reported that Zn exhibits a stimulatory effect on bone formation and mineralization *in vivo* and *in vitro*, decreases the inflammatory response and possesses an antibacterial property.[26-30] There are also several studies on the coating of the metal ion substituted HAP which has been shown to improve its structural stability and cellular biocompatible properties.[31-34] Since bioactive elements, like Sr, Mg, Zn have been found to play important roles in regulating the biological responses, it is of great interest to combine bioactive elements for developing bioactive composite coatings on Ti orthopedic implants to elicit their multidirectional effects on their biological properties.[35]

Although HAP and minerals substituted HAP coatings on implants showed long-term survival there are concerns about their reliability under loads (i.e., long term applications).[36] Possible ways to overcome this lack of mechanical stability could be attained by reinforcing the HAP with reinforcing materials such as zirconia, CNT and alumina, etc.[37-40] CNT, is a prospective reinforcement material for brittle HAP, as it exhibits high Young's modulus and tensile strength.[41] CNT are being broadly researched as reinforcement for improving the fracture toughness and wear resistance of brittle ceramics, such as HAP,[42-44] and Al_2O_3.[45] However, CNT has been found to aid in accelerated bone growth and apatite precipitation and induce bonding and reinforcement with the bone matrix.[46-48] *In vitro* studies have shown the CNT/HAP composites possess improved biocompatibility with osteoblasts and macrophages.[49] However, *in*

vivo response of CNT/HAP composite coated Ti implants in bones has never been explored much. In particular, CNT/M-HAP composite coating on Ti obtained by pulsed electrodeposition is a novel technique which provides desired morphology and offers homogenous distribution of minerals for the bone formation. As this technique possesses advantages like simple operation, high purity of deposits, easy control of the particle-size by adjusting pulse parameters such as pulse on time, pulse off time and current density,[50-52] low cost and compact coating, researchers show more interest on the pulsed electrodeposition of bioceramic coating.[53-58] Also, when the pulsed power is applied to the electrolyte, the mineral ions come closer to the cathode and effectively get deposited homogenously. The mobility of ions takes place in the bulk solution to the surface of the cathode, during the relaxation time, so as to provide homogeneous distribution of mineral ions in the coating which can improve biological properties of implant.[15,20,35,59] The homogenous distribution of mineral ions can lead to the formation of desired morphology for the bone formation.

Based on these issues, our present work is designed to evaluate the *in vitro* biocompatibility of the osteoblast cells on the CNT/M-HAP composite coating and to investigate the effects of pulsed electrodeposited CNT/M-HAP composite coating on implant fixation in femur bones of Wistar rats by *in vivo* histological evaluation for 14 and 28 days of implant insertion. The study of *in vivo* behaviour of the CNT/M-HAP composite coating is the most significant feature of the present work. The obtained results suggested the feasibility of using the as-developed CNT/M-HAP composite coated Ti with enhanced mechanical and biological properties for major load-bearing implant applications.

2. Materials and methods

2.1. Preparation of implants

Sixteen rod shaped implants made of pure Ti (99.9% purity, Sigma-Aldrich, USA) with diameter of 1 mm and length of 12 mm were used in this study for implantation. The implant model was featured by a rod to facilitate a standard method of harvesting bone-implant tissues for histological analyses. Before the coating process, all the implants were grit blasted with aluminium oxide.

2.2. Preparation of M-HAP electrolyte

Analytical grade $Ca(NO_3)_2 \cdot 4H_2O$, $Sr(NO_3)_2 \cdot 6H_2O$, $Mg(NO_3)_2 \cdot 6H_2O$ and $Zn(NO_3)_2 \cdot 6H_2O$ were dissolved in deionized water separately and the solutions were mixed in the ratio of 7:1:1:1, respectively. The $(NH_4)_2HPO_4$ was dissolved in deionized water and both the solutions were mixed to produce the target (Ca+Sr+Mg+Zn)/P ratio of 1.67. The electrolyte was prepared in the N_2 gas atmosphere and the pH of the electrolyte was maintained to 4.7 at 65 °C using thermostat. The electrolyte was magnetically stirred for 2 h at a speed of 180 rpm to maintain uniform concentration. Finally, H_2O_2 (2000 ppm) was added in the electrolyte solution to diminish the formation of H_2 gas bubbles.[60] In addition, pure HAP electrolyte was also prepared using $Ca(NO_3)_2 \cdot 4H_2O$ and $(NH_4)_2HPO_4$ by adopting the same procedure.

2.3. Preparation of CNT/M-HAP electrolyte

Initially, the functionalisation of CNT was performed by dispersing it in the concentrated aqua regia (1:3) under ultrasonic irradiation of 1 h at room temperature (28 ± 1 °C). The mixture was then heated to 110 °C in an oil bath, refluxed, and then cooled to room temperature. The obtained solution was then filtered and the filtrate was washed with deionized water repeatedly until the filtrate became neutral and the final product was dried at 60 °C during 48 h.[61] To the electrolyte of M-HAP (prepared as mentioned in section 2.2), 1 wt% of functionalized CNT was

added by maintaining pH 4.7. The CNT/M-HAP electrolyte solution was exposed to strong ultrasonic treatment for the effective dispersion of CNT during 30 min.

2.4. Pulsed electrodeposition of HAP, M-HAP and CNT/M-HAP on Ti

The electrodeposition was performed in a common three electrode configuration where Ti specimens served as a working electrode, platinum and saturated calomel electrode as counter electrode and reference electrodes, respectively. The deposition was performed for 1 h on Ti specimens in a galvanostatic mode with a constant current density of 1.0 mA cm^{-2}. The pulse on and off time for the deposition was optimized following the author's previous work.[35] The 1 s pulse on and 4 s pulse off time was kept constant with respect to the current density of 1.0 mA cm^{-2} and 0 mA cm^{-2}. Then, the specimens were removed from the electrolyte and washed with deionized water and then sterilized in an autoclave.

2.5. Characterization of coatings

2.5.1. Phase structure and morphological characterization

The functional groups present in the coatings were identified by Fourier transform infrared spectroscopy (FTIR, Bruker Tensor 27) over the wave length range of 4000-400 cm^{-1}. The phase composition of the as-developed coatings was investigated by X-ray diffraction (XRD, Bruker D8 Advance diffractometer) in the 2θ range of 20-60° at a scan rate of 0.02°. Morphological investigations of the coatings were performed using a Field Emission Scanning electron microscope with Oxford EDX, UK, operating at an accelerating voltage of 30.0 kV. The cross sectional SEM analysis of CNT/M-HAP composite coated Ti was also carried out using FESEM and the average thickness of the composite coating was obtained from five measurements at different positions. The elemental analysis and elemental mapping were performed on composite coated Ti using FESEM to examine the distribution of various elements in the composite. The microstructure of the composite coating was also characterized using high

resolution transmission electron microscopy (HRTEM, JEOL JEM 2100 Co., Tokyo, Japan). The samples for HRTEM analysis was prepared by scraping the coating from the Ti substrate and dispersing it in ethanol, followed by the sonication step for 10 min. Then a drop of suspension was deposited on copper coated carbon grid with 200 meshes and the solvent was allowed to evaporate.

X-ray photoelectron spectroscopy (XPS; Omicron Nano-Technology instrument) with a focused monochromatic Al Kα source (1486.6 eV) for excitation was utilized for chemical composition analysis of CNT/M-HAP composite coating. The electron takeoff angle was 54.7° and for all the measurements the analyzer was operated at a constant-energy mode. XPS survey spectrum over a binding energy range of 0-1100 eV was acquired with analyzer pass energy of 50 and 20 eV for high-resolution elemental scans. The vacuum pressure was around 3.5×10^{-10} mbar during spectral acquisition. The data analysis was carried out with EIS-Sphera software provided by the manufacturer. The obtained intensity ratios were converted into atomic concentration ratios by using the sensitivity factors proposed by the manufacturer.

2.5.2. Mechanical characterization

The adhesion strength of the HAP, M-HAP and CNT/M-HAP coatings on Ti implant was carried out by the pull-out test according to the American Society for Testing Materials (ASTM) international standard F1044-05,[62] with five experiments for each sample. The specimens were subjected to tests at a constant cross-head speed using a universal testing machine (Model 5569, Instron).

2.5.3. Inductively coupled plasma atomic emission spectroscopy

The mineral ions release study for the CNT/M-HAP composite coated Ti was performed using the inductively coupled plasma atomic emission spectroscopy (ICP-AES, Thermo Electron

IRIS INTREPID II XSP DUO,USA). The fresh SBF was maintained when the composite coated specimen was immersed in SBF for 1, 4 and 7 days.

2.6. *In vitro* cytotoxicity

Human osteosarcoma MG63 osteoblast-like cells (HOS MG63, ATCC CRL-1427TM) were purchased from National Centre for Cell Sciences (NCCS), Pune, India, and then cultured in standard culture medium (Dulbecco's Modified Eagle Medium (DMEM, GIBCO)), which consisted of a minimal essential medium, supplemented with 10% fetal bovine serum (FBS), and 1% non-essential amino acids (GIBCO). The minimal essential medium was renewed for every two days and then the cultures were maintained in a humidified atmosphere of 5% CO_2, at 37 °C. The osteoblast cultures were separated from the culture flask by incubation with 0.1% trypsin and 0.1% ethylene diamine tetraacetic acid (EDTA) for about 5 min. The viability of HOS MG63 cells colonizing the samples (HAP, M-HAP and CNT/M-HAP coatings) were evaluated using MTT (3-(4,5-dimetyl-2-tiazolyl)-2,5-diphenyl-2H-tetrazolium bromide) assay. To determine the cytotoxicity of the samples at different conditions, HOS MG63 cells were seeded in 12-well plates at 10^4 cells/mL in a humidified 5% CO_2 atmosphere. After 24 h of incubation, MTT solution (in 1 mL serum free medium) was added and then incubated for 4 h at 37 °C in a humidified 5% CO_2 atmosphere. The solution was removed and dimethyl sulfoxide was added to it, and the plate was shaken for 15 min before measuring absorbance at 570 nm (the reference value was 690 nm) on an ELISA microplate reader and then % cell viability was calculated with respect to control as follows,

$$\% \text{ Cell viability} = [A] \text{ Test}/[A] \text{ Control X } 100.$$

2.7. Statistical analysis

The cytotoxicity test was performed for all the coatings in triplicate and repeated three times (mean ± SE). The statistical analysis was performed using analysis of variance (ANOVA)

with Tukey's multiple comparison tests (Prism 5.0 version). The difference observed between samples was considered to be significant at $P < 0.05$.

2.8 *In vivo* evaluation

2.8.1. Animals experimental design and implantation procedures

Sixteen male Wistar rats aged 6 months and weighing approximately 250 g were bred individually in cages under standard climatic conditions (25 °C; 55% humidity; 12 h of light alternating with 12 h of darkness). The care for the animals and its surgical procedure were conducted as being compliant with the guidelines of the Institutional Animal Ethics Committee (IAEC) at Kovai Medical Center Research and Educational Trust, Coimbatore, India (KMCRET/Ph.D/3./2013-2014). The rats were kept staying in identical environments and all were receiving standard rodant diets and pure water.

For the implantation purpose, sixteen Ti implants were separated into four groups: Group-I: uncoated Ti, Group-II: HAP coated Ti, Group-III: M-HAP coated Ti and Group-IV: CNT/M-HAP composite coated Ti. The rats were anesthetized by ketamine (100 mg kg^{-1}) and xylazine (5 mg kg^{-1}) body weight intramuscularly and the implantation was conducted under aseptic condition.[63] The fur was removed at the surgical site and using blunt dissection, the muscles were separated over the femur to expose the periosteum. After dissection of the periosteum, implants were inserted inside the right femur bone by making a 2 mm hole using the drilling machine. The implant sites penetrated into the marrow cavity of the femur. Abundant irrigation with physiologic saline was maintained throughout the drilling to minimize the temperature rise in the bone. Finally, the skin was sutured and was then allowed to recover from anesthesia in a warm environment while being observed. The animals received antibiotics (penicillin) for three postoperative days. The rats were kept on rearing for 14 and 28 days and all animal were monitored twice in a day, especially during the first week after surgery. Two rats

from each group were sacrificed after 14 days and the other rats were sacrificed after 28 days of implantation and specimens were harvested for the histological evaluation.

2.8.2. Histological analysis

Immediately after sacrifice, the left femur with implants were maintained in a 4% neutral formalin buffered solution, then washed, dehydrated in graded ethanol and embedded in methylmethacrylate without decalcification. The bones with the implants were sectioned to a thickness of 1-2 mm, with a low speed diamond saw. For histological observations of rat's bones, sections were also stained with toluidine blue coloration and analyzed by light microscopy.

3. Results

3.1. FTIR

The Fourier transform infrared spectroscopic technique was used for the analysis of functional groups present in HAP, M-HAP and CNT/M-HAP coatings and the corresponding spectra are shown in Fig. 1. The FTIR spectrum for HAP coating is shown in Fig. 1a. The peaks observed at 3444 and 1641 cm^{-1} are due to the stretching and bending modes of adsorbed water. The stretching and bending vibrational modes of hydroxyl (–OH) group were identified at 3564 and 632 cm^{-1}, respectively. The characteristic absorption peaks for phosphate group of HAP are observed at 561 and 602 cm^{-1} (ν_4), 1048 and 1098 cm^{-1} (ν_3) and 962 cm^{-1} (ν_1) which are assigned to P–O bending, asymmetric P–O stretching and symmetric P–O stretching vibrations, respectively. The PO_4^{3-} bending vibration (ν_2) is attributed at 475 cm^{-1}. Figure 1b represents the peaks for M-HAP coating. The characteristic absorption peaks for phosphate group of M-HAP are observed at 558 and 590 cm^{-1} (ν_4), 1017 and 1081 cm^{-1} (ν_3) and 948 cm^{-1} (ν_1), which are assigned to P–O bending, asymmetric P–O stretching and symmetric P–O stretching vibrations, respectively. The peaks observed at 3439 and 1621 cm^{-1} are due to the stretching and bending

modes of absorbed water. The absorption peaks observed at 3587 and 636 cm^{-1} are assigned to the stretching and bending vibration of the OH^- group. This change in the wave numbers of the M-HAP and CNT/M-HAP composite coating in comparison to HAP is due to the difference in the ionic radius of the minerals present in the coatings. Although there are three different mineral ions (Sr^{2+} (radius, 0.112 nm), Mg^{2+} (0.072 nm) and Zn^{2+} (0.074 nm) for Ca^{2+} (0.100 nm)) substituted in the HAP lattice, the shift in the wave numbers is influenced by the greater ionic radius of Sr^{2+} (0.112 nm) substituted into the apatite.[64] In addition to all the above peaks, a strong absorption peak at 1380 cm^{-1} indicates the interaction of CNT and minerals in HAP which confirms the formation of CNT/M-HAP composite coating (Fig. 1c). Thus, FTIR results confirm the formation of HAP, M-HAP and CNT/M-HAP composite coatings.

3.2. XRD

The XRD patterns obtained for HAP, M-HAP and CNT/M-HAP composite coatings are shown in Fig. 2. The diffraction patterns of M-HAP and CNT/M-HAP composite coatings showed that the peaks obtained were shifted towards lower angles when compared to that of HAP (ICDD 09-432).[65] This is due to the substitution of Sr^{2+} (ionic radius, 0.112 nm), Mg^{2+} (ionic radius, 0.072 nm) and Zn^{2+} (ionic radius, 0.074 nm) in the HAP lattice. Though there are three divalent mineral ions substituted for Ca^{2+}, the lower angle shifts are essentially due to the greater ionic radius of Sr^{2+} (0.112 nm) which is substituted into the HAP matrix. In this regard, the main diffraction peaks of CNT/M-HAP obtained are shifted to the left side due to the substitution of mineral ions which occurred by expansion and contraction in the HAP lattices. In addition to the HAP peaks, a diffraction peak at 26.37° is observed that corresponds to graphite crystallographic (002) plane of CNT which is in good agreement with ICDD card No. 41-1487.[66] Thus, from the XRD result, the substitution of mineral ions and the reinforcement of CNT in HAP coatings are confirmed.

3.3. Morphological results and elemental mapping analysis

The HRSEM micrographs of pulsed electrodeposited HAP, M-HAP and CNT/M-HAP composite coatings obtained at 1 s pulse on time and 4 s pulse off time are shown in Fig. 3. The Fig. 3a shows the uniform flake-like structure for HAP coating whereas a sphere like morphology is obtained for the M-HAP coating (Fig. 3b) which covers the entire surface of the implant. The CNT/M-HAP composite coating consisted of fine sphere like particles that fully covered the Ti surface (Fig. 3c). The morphologies of the obtained coatings are well evident from the magnified version of the figures which are given as the insets to the corresponding SEM images (Fig 3(a-c)). The morphological changes may be due to the substitution of mineral ions and reinforcement of CNT in HAP at the prolonged pulse off time. This indicates that the pulsed electrodeposition technique seems to be favorable for the growth of resultant coatings on Ti. The sphere like morphology (Fig. 3c) will be favorable for the effective adhesion and proliferation of cells.[67] Fig. 3d shows the SEM cross-sectional view of the CNT/M-HAP composite coating on Ti. The composite coating is found to be compact and dense with thickness of about 18.1 μm which revealed that the composite coating is bonded tightly on the Ti substrate.

The elemental mapping of CNT/M-HAP composite coating indicated the ubiquitous presence of Ca, Sr, Mg, Zn, P, O and C at areas of differential concentration (Fig. 4a-g). The Sr, Mg and Zn distribution corresponds well to the Ca and P distributions, confirming the substitution of the mineral ions into the HAP lattice. In addition to these, the distribution of carbon in the composite coating was found which revealed the reinforcement of CNT in M-HAP composite. The EDS spectrum of the CNT/M-HAP composite coating shows the presence of Ca, Sr, Mg, Zn, P, O and C (Fig. 4h), indicating the existence of CNT and minerals in HAP composite coating. Thus, the homogenously distributed mineral ions and the reinforced CNT particles can be observed upon EDS mapping analysis.

The TEM micrograph of the CNT/M-HAP composite coating is presented in Fig. 5. The tubular structure of CNT (the walls of the tubular structure is marked) in CNT/M-HAP coating confirmed the presence of CNT through the high resolution TEM result. Furthermore, the spherical particles of M-HAP strongly bounded to the surface of CNT evidences that the CNT acts as a better reinforcing material for M-HAP.

3.4 X-ray photoelectron spectroscopic study

XPS survey spectrum identified Ca, P, Sr, Mg, Zn, C, and O as the major constituents of the composite coating on Ti (Fig. 6a) and the corresponding deconvolution spectra are also shown in Fig. 6b-g. Binding energies of the obtained peaks and the atomic ratio of the ions in the composite coatings are given in Table 1. The binding energies of $Ca2p_{3/2}$, O1s, and P2p, were 347.2, 530.8 and 133.3 eV, respectively, which are in good agreement with the reported values of HAP.[68] In Fig. 6e, the peak at 133.4 eV was an overlap of Sr3d and P2p because the $Sr3d_{5/2}$ (133.4 ± 0.5 eV) and P2p (133.3 eV) lines were closely located. The amount of C present is most likely due to the reinforcement of CNT. The XPS data support the formation of CNT/M-HAP composite coating on Ti.

3.5. Adhesion strength of the coatings

Microstructural changes eventually result in a change in mechanical properties. To determine changes in mechanical properties with CNT reinforcement and the substitution of mineral ions, the pull out tests are performed and the results are discussed below. The adhesion strength of the resultant coatings at 1 s pulse on time and 4 s pulse off time was determined by standard adhesive testing (ASTM F1044-05). Adhesion of the CNT/M-HAP composite coating onto the Ti surface is one of the most significant properties for the *in vivo* implantation. The adhesion strength of the HAP, M-HAP and CNT/M-HAP coatings on Ti, respectively was evaluated and is shown in Fig. 7. The adhesion strength for the HAP coating was about 17.71 ±

0.4 MPa, similarly, the M-HAP coating on Ti showed adhesion strength of 20.5 ± 0.6 MPa. The CNT/M-HAP composite coating showed 28.23 ± 0.9 MPa which exhibits high adhesion compared with other coatings. The obtained value (28.23 ± 0.9 MPa) is more or less similar to the adhesion value of the CNT/HAP coating obtained by aerosol deposition (29.0 ± 1.1 MPa) reported by Hahn et al.[49] Thus, it is concluded that the reinforcement of CNT and the substitution of minerals in HAP has improved the adhesion strength between the resultant composite coating and Ti metal.

3.6. ICP-AES analysis

The mineral ions release from the CNT/M-HAP composite coated Ti was evaluated from the ICP-AES analysis by soaking the composite coated Ti in SBF solution for 1 to 7 days and the results are shown in Fig. 8. It is clear from the figure that, the release of mineral ions from CNT/M-HAP composite coating for the one day was greater than those obtained at other days of immersion. In particular, the Ca ion concentration in the solution increased rapidly as the immersion time increased from 0 to 1 day. Similarly, the release of other minerals like Sr, Mg, Zn and phosphate ions in the solution also slightly increased as shown in Fig. 8. But as the immersion time increases from 4 to 7 days, the concentration of mineral ions release slightly decreased which supports for the apatite growth.

3.7. *In vitro* cytotoxicity results

The effect of HAP, M-HAP and CNT/M-HAP coatings on the proliferation of HOS MG63 cells at different days of incubation such as 1 day, 4 days and 7 days is displayed in Fig. 9. The optical images of the HAP, M-HAP and CNT/M-HAP coatings showed good cell proliferation at day 1 without any dead cells (Fig. 9a, d and g). Further increasing the incubation time to 4 (Fig. 9b, e and h) and 7 (Fig. 9c, f and i) days, a better cell proliferation was obtained for all the coatings. In particular, the composite coating results noticeable cell viability

at 7 days of incubation, which indicates that the CNT/M-HAP induces the cell growth rather than the toxicity against HOS MG63 osteoblast cells.

In addition, the % of cell viability for all the coatings is displayed in Fig. 10. The relative cell viability for the biomaterials should be greater than 75% of the control and it is defined as nontoxic according to the ISO standard 10993-5.[69] This concept was proved by Gopi et al., in his previous report that the reinforcement of CNT into the HAP moiety did not affect the non toxic nature of the biomaterial.[70] The obtained coatings showed significant % of cell viability at different days of incubation, in which the M-HAP and CNT/M-HAP coatings showed ~99 % of cell growth at the day of incubation 7. This result elevates the promising opinion about the bioceramic material for improved orthopedic applications.

3.8. In vivo evaluation

3.8.1. Clinical results

A total of 16 animals were used for this study. Each animal received only one type of implant in order to avoid systemic responses. Clinical results showed that none of the animals died during surgery or postoperation. Rats were able to walk without any disabilities after the implantation surgery. No infection, no disunion of the scar, and a complete range of motions of the knee joint were observed. It is observed from Fig. 11 that after dissection and retrieval of all parts of the femoral bone with knee joint no infected tissues were found. The radiographs of the rat femoral bone before and after implantation are shown in Fig. 12.

The implants from group I (bare Ti), II (HAP coated Ti), III (M-HAP coated Ti) and IV (CNT/M-HAP composite coated Ti) were well-positioned inside the external femoral condyle. We also observed good osseointegration (no osteolysis around implants) or no specific periostal reactions (sign of infection) around the four groups of implants in the rats and particularly improved osseointegration was observed around CNT/M-HAP composite coated Ti.

3.9. Histological observations

Figure 13 shows the representative histological observations of group I, II, III, and IV implants embedded in rats. Bone tissue exhibited newly grown bone at two and four weeks of post implantation. The qualitative analysis at two weeks indicated the presence of connective tissue on implant for all groups tested. Four weeks after implantation, all coated implants (Group: II, III and IV) exhibited extensive trabecular bone formation than the non-coated Ti implants. The group IV displays more matured bone with numerous osteoblast-like cells seen around the implant which shows the improved amount of bone formation on Ti. A noticeable difference in the bone formation was observed for M-HAP coated Ti when compared to HAP coated Ti, whereas for CNT/M-HAP composite coating, the presence of osteoid and fibrocollagenous stroma was observed. Generally, the osteoblasts begin the process of forming bone tissue by secreting the osteoid as several specific proteins. When the osteoid becomes mineralized, they develop into new bone tissue along with the adjacent bone cells. This supports that the addition of CNT has not caused any adverse effect or inflammatory reaction. But, the group I (i.e.) uncoated Ti implant exhibited slightly reduced bone formation among the other coated implants. This study clearly envisioned that, the CNT/M-HAP composite coating accelerates osseointegration of Ti implant, which eventually improves the fibrocollageous stroma around the implant material.

4. Discussion

The Bone has the extraordinary capacity to get cured without any scar formation, but this process fails in patients with large bone defects which require clinical observation. In recent years, there is a growing demand for ‘ideal bone graft’. An ideal bone graft must possess good biocompatibility and better osseointegration, osteoconduction, osteoinduction and osteogenic property. Ti implants are widely used in the field of biomedical implants, as dental and

orthopedic implants.[71] Despite the extensive use of Ti, the osseointegration of Ti implants in medically compromised patients (especially in orthopedic patients) still remains a challenge.[72] For this purpose, we have focused on the successful development of bioceramic composite coating on Ti with the combination of CNT reinforcement and the substitution of minerals in HAP and investigated their biological effects on the proliferation of HOS MG63 cells and *in vivo* response in the Wistar rats. We have also observed the adhesion strength of the composite coating on Ti. Although good biocompatibility, osteoconductivity and bone bonding ability of HAP and CNT/HAP coating have been found out *in vivo*, no animal experimentation investigating the simultaneous effect of reinforcement of CNT and the substitution of minerals in HAP has been studied. Thus, this study might be the first report indicating the enhanced osseointegration of CNT/M-HAP composite coated Ti implants in rats, a widely used animal model. The results from our studies showed that the specific combination of CNT and bioactive ions (Sr, Mg, Zn) in HAP significantly improved the mechanical and biological properties.

The FTIR spectra confirmed the formation of HAP, M-HAP and CNT/M-HAP composite coatings obtained by pulsed electrodeposition and no other impurities were identified. The spectra obtained for M-HAP and CNT/M-HAP coatings showed the peaks similar to that obtained for HAP coating but with a slight change in the wave numbers. The change in the wavenumbers is due to the difference in the ionic radius of the minerals (Sr^{2+}, Mg^{2+}, Zn^{2+}) substituted in HAP. Similarly the peak at 1380 cm^{-1} indicates the interaction of Ca^{2+}, Sr^{2+}, Mg^{2+}, Zn^{2+} (in M-HAP) with COO^{-} group of oxidised CNT, thus confirming the formation of CNT/M-HAP composite coating.

The XRD pattern of CNT/M-HAP composite coatings was similar to that of HAP but with the reinforcement of CNT and the substitution of minerals in HAP there appeared an additional peak at 26.37° and a slight shift in the peak values towards lower diffraction angles,

respectively. The slight shift towards lower diffraction angles is attributed to the crystal lattice distortion of HAP that has occurred as a result of substitution of mineral ions such as Sr^{2+}, Mg^{2+} and Zn^{2+} in HAP.

SEM observations of the HAP, M-HAP and CNT/M-HAP coatings obtained at 4 s pulse on and 1 s pulse off time revealed changes in the size and morphology. The morphology of the HAP, M-HAP and CNT/M-HAP coatings varied from flakes like to small sphere like structure as evidenced in Fig. 3a-c. The small-sphere like morphology of CNT/M-HAP coating with the thickness of about 18.1 μm is favorable for the adhesion and proliferation of cells.[67,73] The EDS analysis supported the elemental composition of the CNT/M-HAP composite coating on Ti. In addition to this, the EDS mapping presented the distribution of Ca, Sr, Mg, Zn, P and O in the composite coating. No sign of coating disintegration was observed from SEM and EDS analyses. From the above results it is observed that the pulsed electrodeposition ensured the homogenous distribution of mineral ions in the composite that has resulted in a compact coating with better bioresistivity and good biocompatibility.[35]

The atomic ratio and the binding energy of the carbon nanotubes reinforced minerals substituted hydroxyapatite composite coating is clearly revealed by the XPS analysis and is also well evident from the Table 1. Adhesion strength of the coatings was tested to make sure that no debris particles generated during implant insertion. Among the coatings, the CNT/M-HAP composite coating exhibited enhanced adhesion strength which is due to the reinforcement of CNT and also the substituted minerals in the coatings. The release of mineral ions in the as-developed CNT/M-HAP composite coating is decreased as increasing the immersion days which evidences for the formation of apatite on the composite coated implant.

The duration of culturing of cells on the materials *in vitro* prior to implantation is an imperative aspect that ensures the success of coating. The *in vitro* cell viability of the prepared

coatings was investigated using MTT assay on HOS MG63 cell line. Cells cultured on all the coatings such as HAP, M-HAP and CNT/M-HAP at 1, 4 and 7 days of incubation presented a cell proliferation activity similar to those observed in control cultures. Hence it is evident that, CNT/M-HAP coating has a significant effect on osteoblastic cell proliferation, since Sr, Mg and Zn are known to influence the activity of bone cells.[12,35,74] This clearly evidences that the proper distribution of minerals substitution in HAP and CNT in M-HAP plays an important role in improving the biological performance of the coating.[35] Therefore, the results suggest that the incorporation of CNT and minerals into the HAP would result with the enhanced cytocompatibillity and better cell viability than the HAP coated and uncoated Ti specimens, and hence the as-prepared CNT/M-HAP composite coated Ti has great potential to be used for orthopedic applications.

To evaluate the biological response of HAP, M-HAP and CNT/M-HAP coated in Ti implants, a rat femur implantation model was used. In the literature, different time periods were used for studying the implant osseointegration and the animals are killed after 2 weeks,[75] 4 weeks,[76] 6 weeks,[77] and 3 months.[78] In our study, we have evaluated implant fixation at 14 and 28 days after implantation to assess the static and active process of the bone/implant interaction (osseointegration). Our *in vivo* results were same for all the rats, with no side effects, no osteolysis and with a good osseointegration for CNT/M-HAP composite coating. Clinical and histological observations described above indicate that CNT reinforcement and substitution of minerals in HAP promotes the formation of the new bone without any detrimental effect. The microscopic appearance of the CNT/M-HAP composite coatings showed mature bony formation and marrow spaces that reveals the normal histology of rat femur. The composite coating showed good response when compared to other groups. CNT/M-HAP composite coatings did not induce necrosis or inflammatory reactions,[45] but shows normal bone tissue

formation. Our promising results are attributed to the substitution of minerals like Sr, Mg, Zn in HAP that stimulate osteoblast proliferation and also the presence of CNT that accelerate bone growth, and inhibit osteoclastic bone resorption.[35,49] Thus, the results demonstrated that the osseointegration of the implant material that challenge the quality and duration for the surgeons could be improved by the substitution of minerals and reinforcement of CNT in HAP. We have used animal model to investigate the bone-implant osseointegration of CNT/M-HAP composite coated Ti. However, further investigations *in vivo* are needed for simulating implant integration under a complex clinical condition.

5. Conclusion

In this study, we developed CNT reinforced mineralized HAP composite coating on Ti metal using pulsed electrodeposition method and confirmed its biocompatibility and adhesion strength. The composite coating of CNT/M-HAP was homogeneous, and they strongly adhered to the Ti substrate without any deformation of the material. Also the composite coating exhibited improved cytocompatibillity and bioactivity due to the co-effect of substitution of minerals and reinforcement of CNT into the HAP. The CNT/M-HAP coating on Ti facilitated good proliferation of cultured HOS MG63 cells *in vitro*. The small-sphere like morphology of CNT/M-HAP coating is favorable for the adhesion and proliferation of cells and the elemental mapping evidenced for the homogenous distribution of mineral ions and the reinforcement of CNT in CNT/M-HAP composite coating. The promising results of histological observations that showed good osseointegration indicated the beneficial effect of CNT/M-HAP coating on implant fixation in Wistar male rats. These results have paved the way for the CNT/M-HAP composite coated Ti to be used as a clinically applicable implant material in the near future leading to a faster recovery.

Acknowledgements

One of the authors (D. Gopi) acknowledges major financial support from the Indian Council of Medical Research (ICMR, IRIS ID no. 2010-08660, Ref. no. 5/20/11(Bio)/10-NCD-I), Department of Science and Technology, New Delhi, India (DST-TSD, Ref. no. DST/TSG/NTS/2011/73, DST-EMEQ, Ref. no. SB/ EMEQ-185/2013 and CSIR, Ref. no. 01(2547)/11/EMR-II, Dated:12.12.2011). Also, D. Gopi acknowledges the UGC (Ref. no. F. 30-1/2013 (SA-II)/RA-2012-14-NEW-SC-TAM- 3240 for Research Award.

Notes and references

[1] W.W. Thein-Han and R.D.K. Misra, *Acta Biomater.*, 2009, **5**, 1182-1197.

[2] G. Chiara, F. Letizia, F. Lorenzo, S. Edoardo, S. Diego and S. Stefano, *Int. J. Mol. Sci*., 2012, **13**, 737-757.

[3] H.M. Kim, F. Miyaji, T. Kokubo and T. Nakamura, *J. Biomed. Mater. Res*., 1996, **32**, 409-417.

[4] H. Kato, T. Nakamura, S. Nishiguchi, Y. Matsusue, M. Kobayashi and T. Miyazaki, *J. Biomed. Mater. Res*., 2000, **53**, 28-35.

[5] T. Kokubo, F. Miyaji, H.M. Kim and T. Nakamura, *J. Am. Ceram. Soc*., 1996. **79**. 1127-1129.

[6] J.V. Rau, I. Cacciotti, A.D. Bonis, M. Fosca, V.S. Komlev and A. Latini, *Appl. Surf. Sci*., 2014, **307**, 301-305.

[7] G. Manivasagam, U.K. Mudali, R. Asokamani and B. Raj, *Corros. Rev.,* 2003, **21**, 125-159.

[8] D. Gopi, J. Indira, L. Kavitha, S. Kannan and J.M.F. Ferreira, *Spectrochim Acta. Part A,* 2010, **77**, 545-547.

[9] Y. Huang, X. Jin, X. Zhang, H. Sun, J. Tu and T. Tang, *Biomaterials*, 2009, **30**, 5041-5048.

[10] D. Gopi, P.R. Bhalaji, V.C.A. Prakash, A.K. Ramasamy, L. Kavitha and J.M.F. Ferreira, *Curr. Appl. Phy.,* 2010, **11**, 590-593.

[11] S.V. Dorozhkin and M. Epple, *Angew. Chem. Int. Ed. Engl*., 2002, **41**, 3130-3146.

[12] D. Gopi, S. Nithiya, E. Shinyjoy and L. Kavitha, *Spectrochim Acta. Part A*, 2012, **92**, 194-200.

[13] J. Li, Y. Song, S. Zhang, C. Zhao, F. Zhang and X. Zhang, *Biomaterials,* 2010, **31**, 5782-5788.

[14] D. Gopi, S. Sathishkumar, A. Karthika and L. Kavitha, *Ind Eng Chem Res.,* 2014, **42**, 20145-20153.

[15] D. Gopi, S. Ramya, D. Rajeswari, P. Karthikeyan and L. Kavitha, *Colloids Surf. A,* 2014, **451**, 172-180.

[16] E.S. Thian, J. Huang, S.M. Best, Z.H. Barber and W. Bonfield, *Biomaterials*, 2005, **26**, 2947-2956.

[17] T.C. Brennan, M.S. Rybchyn, W. Green, S. Atwa, A. D. Conigrave and R.S. Mason, *Br. J. Pharmacol*., 2009, **157**, 1291-1300.

[18] D. Gopi, D. Rajeswari, S. Ramya, M. Sekar, R. Pramod and J. Dwivedi, *Appl. Surf. Sci*., 2013, **286**, 83-90.

[19] J. E. Fonseca, *Rheumatology,* 2008, **47**, iv17-19.

[20] D. Rajeswari, D. Gopi, S. Ramya and L. Kavitha, *RSC Adv*., 2014, **4**, 61525-61536.

[21] L. Li, J. Gao and Y. Wang, *Surf. Coat. Technol*., 2004, **185**, 92-98.

[22] J. Takaya, H. Higashino and Y. Kobayashi. *Magnes Res.,* 2004, **17**, 126-136.

[23] Y. Yamasaki, Y. Yoshida, M. Okazaki, A. Shimazu, T. Kubo and Y. Akagawa, *Biomaterials*, 2003, **24**, 4913-4920.

[24] M.P. Staiger, A.M. Pietak, J. Huadmai and G. Dias, *Biomaterials*, 2006, **27**, 1728-1734.

[25] W.L. Suchanek, K. Byrappa, P. Shuk, R.E. Riman, V.F. Janas and K.S.T. Huisen, *Biomaterials*, 2004, **25**, 4647-4657.

[26] M. Yamaguchi, H. Oishi and Y. Suketa, *Biochem. Pharmacol.,* 1987, **36**,4007-4012.

[27] X. Wang, A. Ito, Y. Sogo, X. Li and A. Oyane, *Acta Biomater*., 2010, **6**, 962-968.

[28] A. Ito, K. Ojima, H. Naito, N. Ichinose and T. Tateishi, *J. Biomed. Mater. Res.,* 2000, **50**, 178-183.

[29] E. Jallot, J-M. Nedelec, A.S. Grimault, E. Chassot, A. Grandjean-Laqueriere, P. Laquerriere and D. Laurent-Maquin *Colloids Surf. B,* 2005, **42**, 205-210.

[30] F. Velard, D. Laurent-Maquin, J. Braux, C. Guillaume, S. Bouthors and E. Jallot, J.-M. Nedelec, A. Belaaouaj and P. Laquerriere, *Biomaterials*, 2010, **31**, 2001-2009.

[31] M. Sato, M.A. Sambito, A. Aslani, N. M. Kalkhoran, E. B. Slamovich and T.J. Webster, *Biomaterials,* 2006, **27**, 2358-2369.

[32] K. Cheng, W. Weng, H. Wang and S. Zhan, *Biomaterials,* 2005, **26**, 6288-6295.

[33] D. Gopi, S. Ramya, D. Rajeswari, M. Surendiran and L. Kavitha, *Colloids Surf. B,* 2014, **114**, 234-240.

[34] D. Gopi, N. Murugan, S. Ramya and L. Kavitha, *J. Mater. Chem. B*, 2014, **2**, 5531-5540.

[35] D. Gopi, A. Karthika, S. Nithiya and L. Kavitha, *Mater. Chem. Phys.,* 2014, **144**, 75-85.

[36] J. J. Lee, L. Rouhfar and O.R. Beirne, *J. Oral Maxillofac. Surg.,* 2000, **58**, 1372-1377.

[37] J. Li, H. Liao and L. Hermansson, *Biomaterials*, 1996, **17**, 1787-1790.

[38] J. Li, B. Fartash and L. Hermansson, *Biomaterials*,1995, **16**, 417-422.

[39] A.A. White, S. M. Best and I. A. Kinloch, *Int. J. Appl. Ceram. Technol.,* 2007, **4**, 1-13.

[40] K. Balani, R. Anderson, T. Laha, M. Andara, J. Tercero and E. Crumpler, A. Agarwal, *Biomaterials*, 2007, **28**, 618-624.

[41] D. Lahiri, A.P. Benaduce, F. Rouzaud, J. Solomon, K. Keshri, L. Kos and A. Agarwal, *J. Biomed. Mater. A,* 2011, **96**, 1-12.

[42] K. Balani, Y. Chen, S.P. Harimkar, N.B. Dahotre and A. Agarwal, *Acta Biomater.,* 2007, **3**, 944-951.

[43] D. Lahiri, V. Singh, A. K. Keshri, S. Seal and A. Agarwal, *Carbon*, 2010, **48**, 3103-3120.

[44] X. Wang, N.P. Padture and H. Tanaka, *Nat. Mater.* 2004, **3**, 539-544.

[45] Y. Usui, K. Aoki, N. Narita, N. Murakami, I. Nakamura, K. Nakamura, H. Yamazaki, H. Horiuchi, H. Kato, S. Taruta, Y.A. Kim, M. Endo and N. Saito, *Small,* 2008, **4**, 240-246.

[46] L.P. Zanello, B. Zhao, H. Hu and R. C. Haddon, *Nano, Lett.,* 2006, **3**, 562-567.

[47] L. Niu, H. Kua and D. H. C. Chua, *Langmuir*, 2010, **26**, 4069-4073.

[48] T. Kasai, S. Matsumura, T. Iizuka, K. Shiba, T. Kanamori, K. Yadasaka, S. Iijima, A. Yokoyama, *Nanotechnol*., 2011, 22, 065102-065109.

[49] B. D. Hahn, J. M. Lee, D. S. Park, J. J. Choi, J. Ryu, W. H. Yoon, B.-K. Lee, D.-S. Shin and H.-E. Kim, *Acta Biomater*., 2009, **5**, 3205-3214.

[50] J. Tang and K. Azumi, *Electrochim. Acta*, 2011, **56**, 1130-1137.

[51] Z.S. Seyedraoufi and S. Mirdamadi, *Mater. Chem. Phys*., 2014, **148**, 519-527.

[52] D. Gopi, J. Indira and L. Kavitha, *Surf. Coat. Technol*., 2012, **206**, 2859-2869.

[53] R. Drevet, H. Benhayounea, L. Worthama, S. Potirona, J. Dougladeb and D.L. Maquina, *Mater. Character*., 2010, **61**, 786-795.

[54] T. Frade, V. Bouzon, A. Gomes and M.I.S. Pereira, *Surf. Coat. Technol.,* 2010, **204**, 3592-3598.

[55] P. Wan, X. Qiu, L. Tan, X.M. Fan and K. Yang, *Ceram. Int.*, 2015, **41**, 787-796.

[56] H. Adelkhani andM.R. Arshadi, J. *Alloys Compd*., 2009, **476**, 234-237.

[57] H.X. Wang, S.K. Guan, X. Wang, C.X. Ren and L.G. Wang, *Acta Biomater*., 2010, **6**, 1743-1748.

[58] R. Drevet and H. Benhayoune, *Mater. Sci. Eng. C*, 2013, **33**, 4260-4265.

[59] A. Kar, K.S. Raja and M. Misra, *Surf. Coat. Technol*., 2006, **201**, 3723-3731.

[60] D. Gopi, A. Karthika, M. Sekar, L. Kavitha, R. Pramod and J. Dwivedi, *Mater. Lett.,* 2013, **105**, 216-219.

[61] D.C. Wu, L. Shen, J.E. Low, S. Y. Wong, X. Li, W. C. Tjiu, Y. Liu, C.B. He, *Polymer*, 2010, **51**, 2155-2160.

[62] ASTM standard F 1044-05. ASTM International, West Conshohocken, PA.

[63] S. Abiraman, H.K. Varma, P.R. Umashankar and A. John, *Biomaterials*, 2002, **23**, 3023-3031.

[64] Z.Y. Li, W.M. Lam, C. Yang, B. Xu, G.X. Ni, S.A. Abbah, K.M.C. Cheung, K.D.K. Luk and W.W. Lu, *Biomaterials,* 2007, **28**, 1452-1460.

[65] S.R. Kim, J.H. Lee, Y.T. Kim, D.H. Riu, S.J. Jung, Y.J. Lee, S.C. Chung and Y.H. Kim, *Biomaterials*, 2003, **24**, 1389-1398.

[66] G.M. Neelgund and A. Oki, *J. Nanosci. Nanotechnol.,* 2011, **11**, 3621-3629.

[67] Y. Ito, *Biomaterials,* 1999, **20**, 2333-2342.

[68] W.J. Landis and J.R. Martin, *J. Vac. Sci. Technol. A*, 1984, 2, 1108-1111.

[69] M. Zhang, C. Wu, K. Lin, W. Fan, L. Chen, Y. Xiao and J. Chang *J. Biomed. Mater. Res. Part A*, 2012, **100A**, 2979-2990.

[70] D. Gopi, E. Shinyjoy, M. Sekar, M. Surendiran, L. Kavitha and T.S. Sampath Kumar, *Corros. Sci.,* 2013, **73**, 321-330.

[71] Y.W. Gu, K.A. Khor and P. Cheang, *Biomaterials*, 2003, **24**, 1603-1611.

[72] R. Family, M. Solati-Hashjin, S.N. Nik and A. Nemati, *Caspian J. Intern. Med.,* 2012, **3**, 460-465.

[73] D.M. Brunette and B. Chehroudi, *J. Biomech. Eng.,* 1999, **121**, 49-57.

[74] D. Gopi, A. Karthika, D. Rajeswari, L. Kavitha, R. Pramod and J. Dwivedi, *RSC Adv.,* 2014, **4**, 34751-34759.

[75] P. Tengvall, B. Skoglund, A. Askendal and P. Aspenberg, *Biomaterials,* 2004, **25**, 2133-2138.

[76] A. De Ranieri, A.S. Virdi, S. Kuroda, S. Shott, R.M. Leven and N.J. Hallab, *Bone*, 2005, **37**, 55-62.

[77] Y. Gabet, D. Kohavi, T. Kohler, M. Baras, R. Muller and I. Bab, *J. Bone Miner. Res.,* 2008, **23**, 48-57.

[78] Y. Gao, S. Zou, X. Liu, C. Bao and J. Hu, *Biomaterials,* 2009, **30**, 1790-1796.

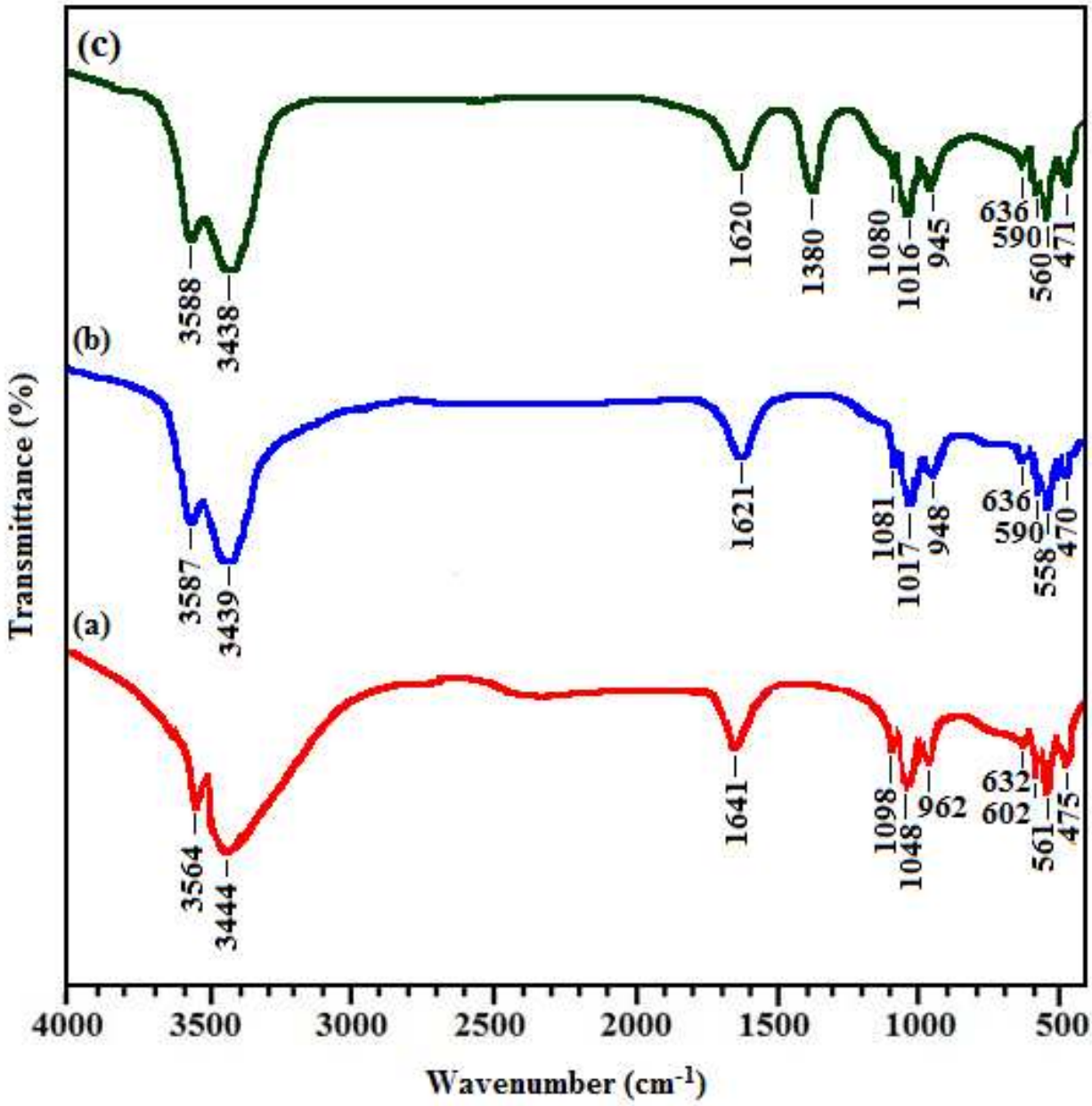

Fig. 1 FTIR spectra of (a) HAP, (b) M-HAP and (c) CNT/M-HAP coatings.

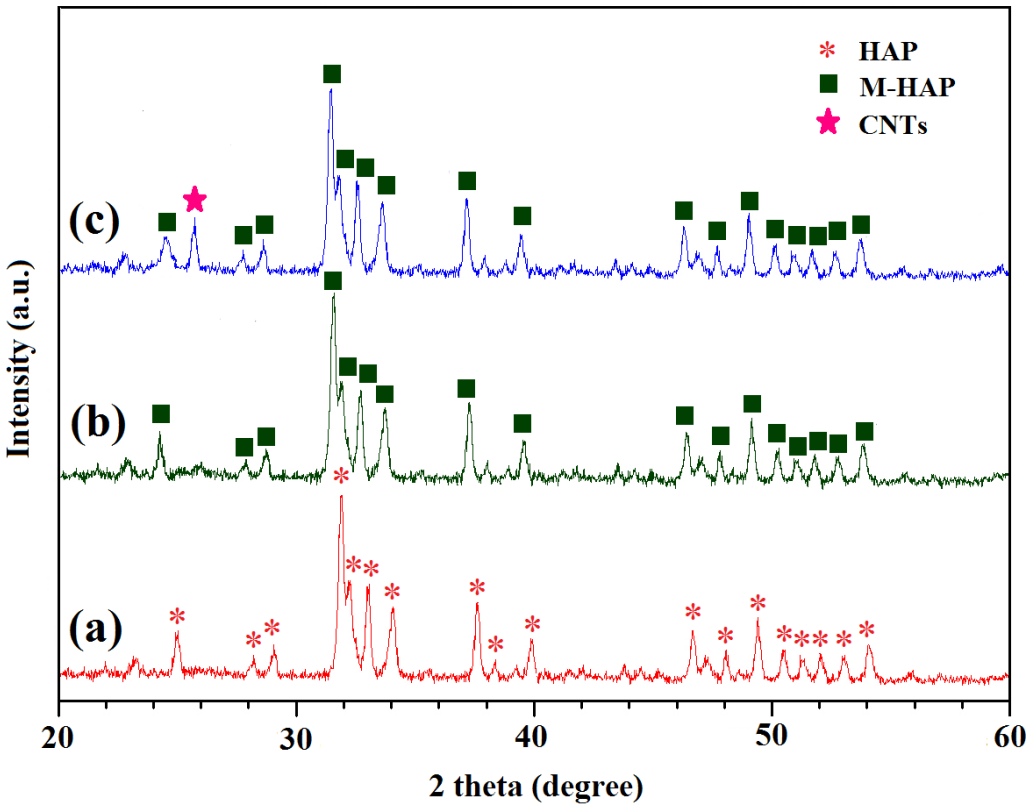

Fig. 2 XRD patterns for (a) HAP, (b) M-HAP and (c) CNT/M-HAP coatings.

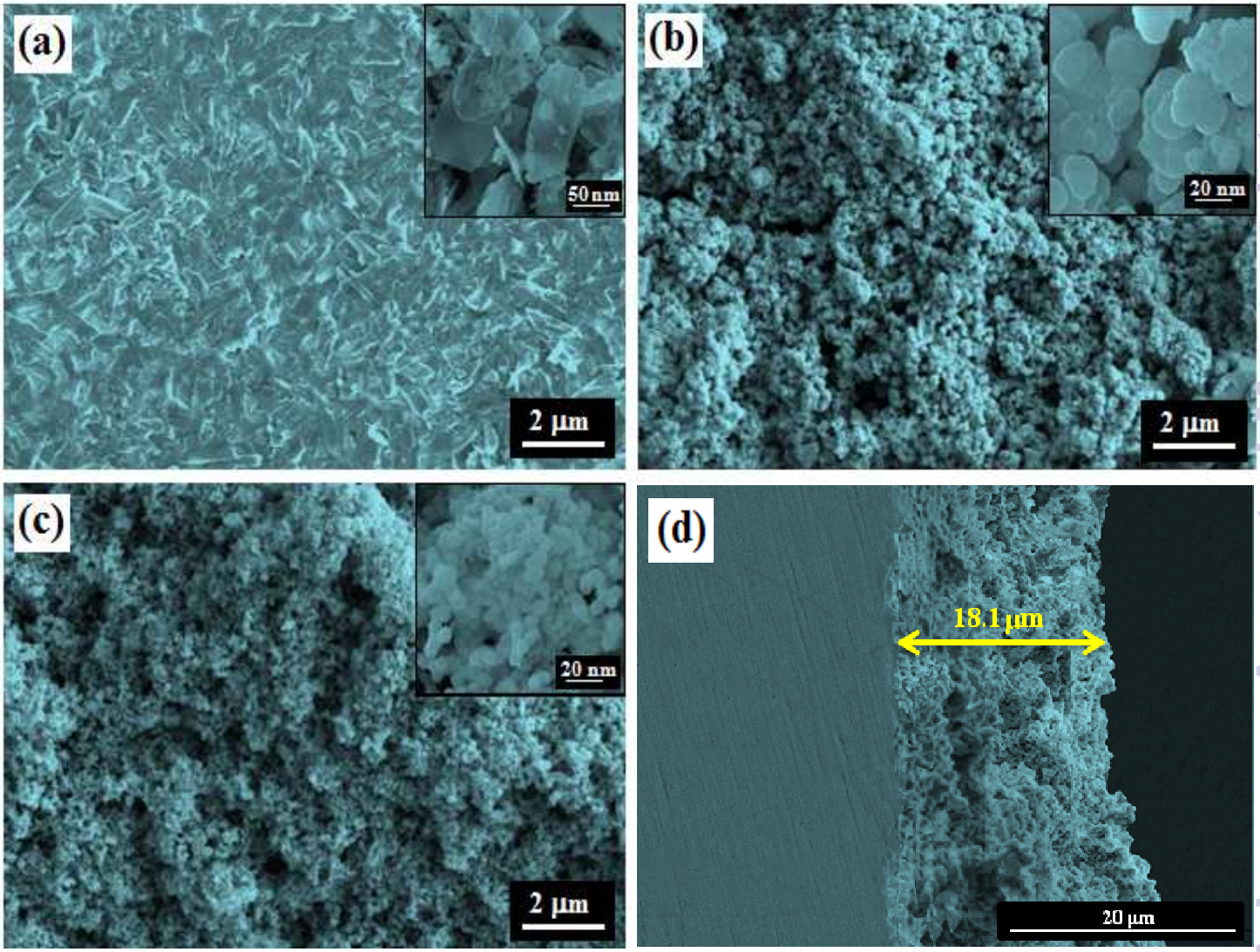

Fig. 3 SEM images of (a) HAP, (b) M-HAP, (c) CNT/M-HAP coatings on Ti implant, and (d) cross sectional SEM image of CNT/M-HAP coating on Ti.

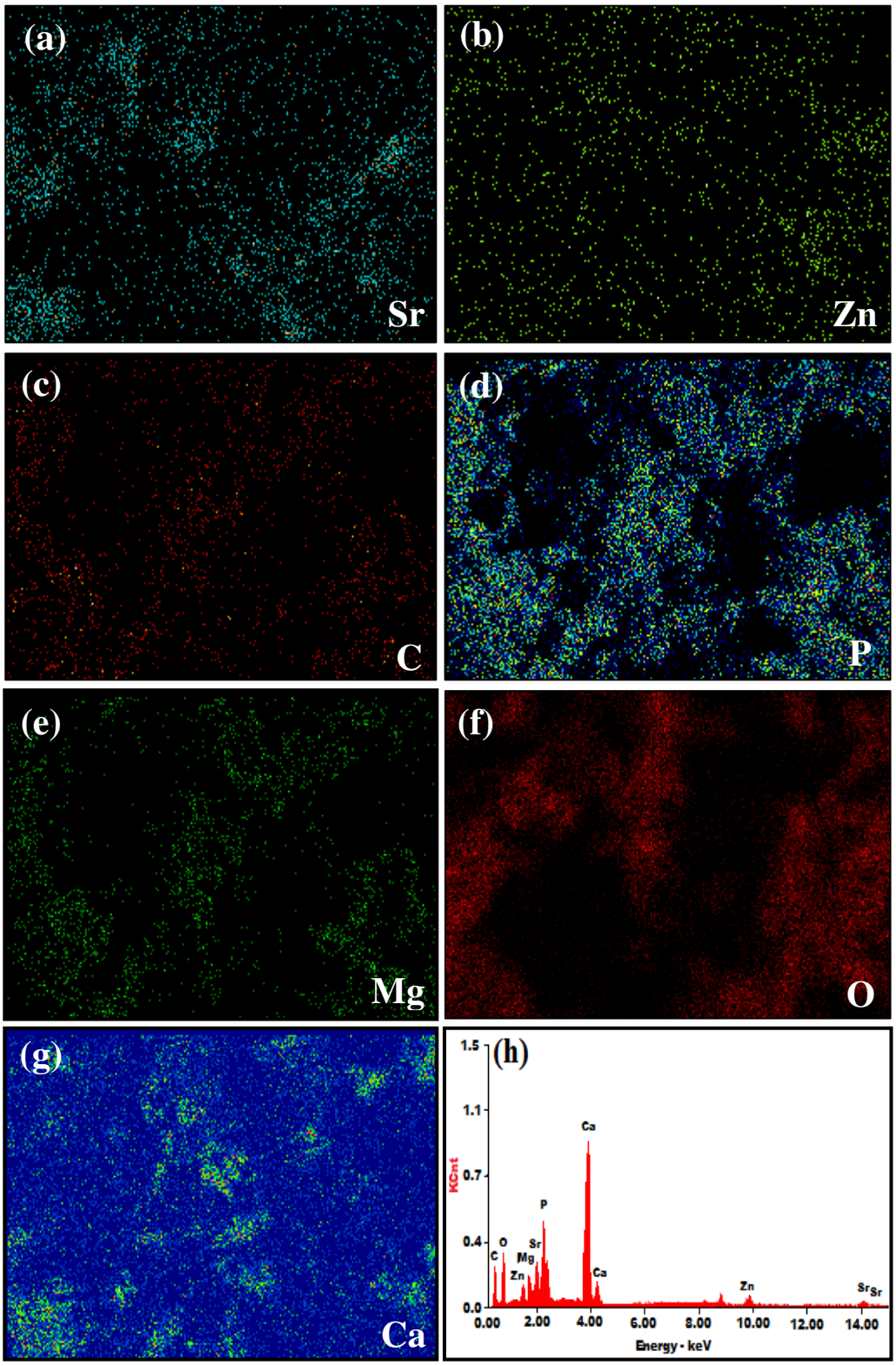

Fig. 4 EDS mapping showing elements of (a) Sr, (b) Zn, (c) C, (d) P, (e) Mg, (f) O, (g) Ca and (h) EDS spectrum of CNT/M-HAP composite coating.

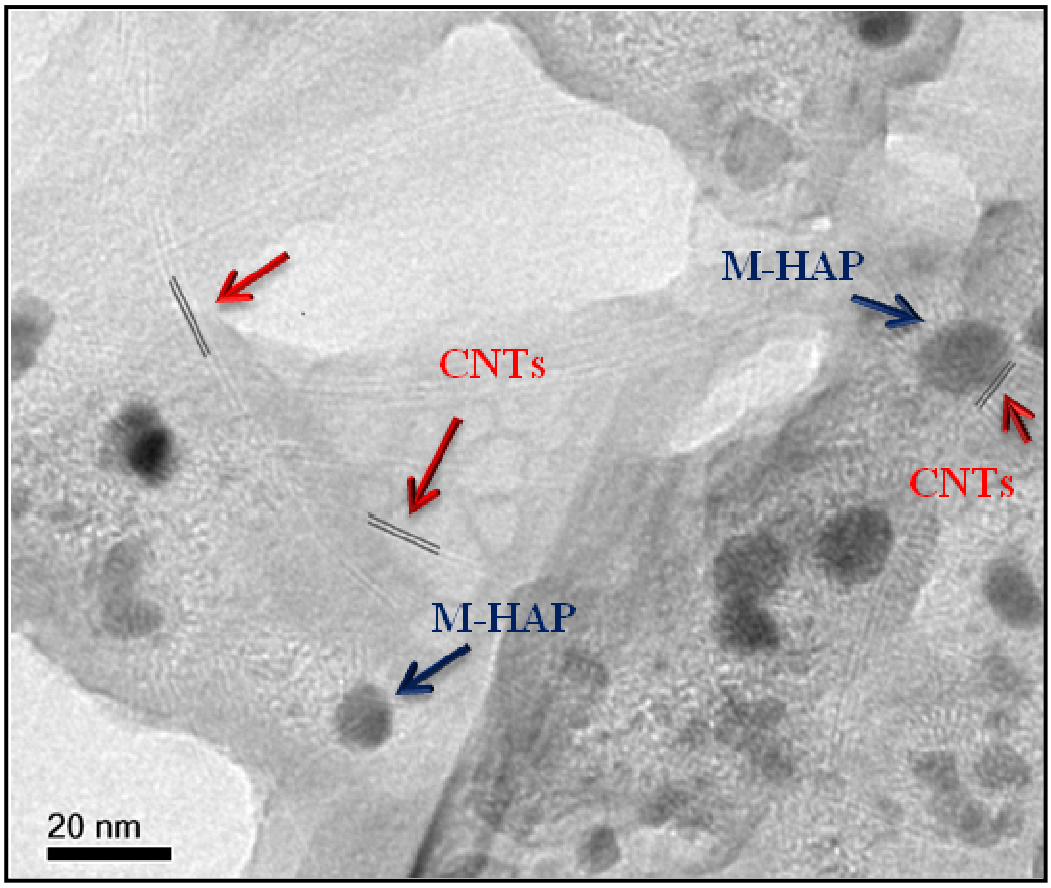

Fig. 5 TEM micrograph of CNT/M-HAP composite coating.

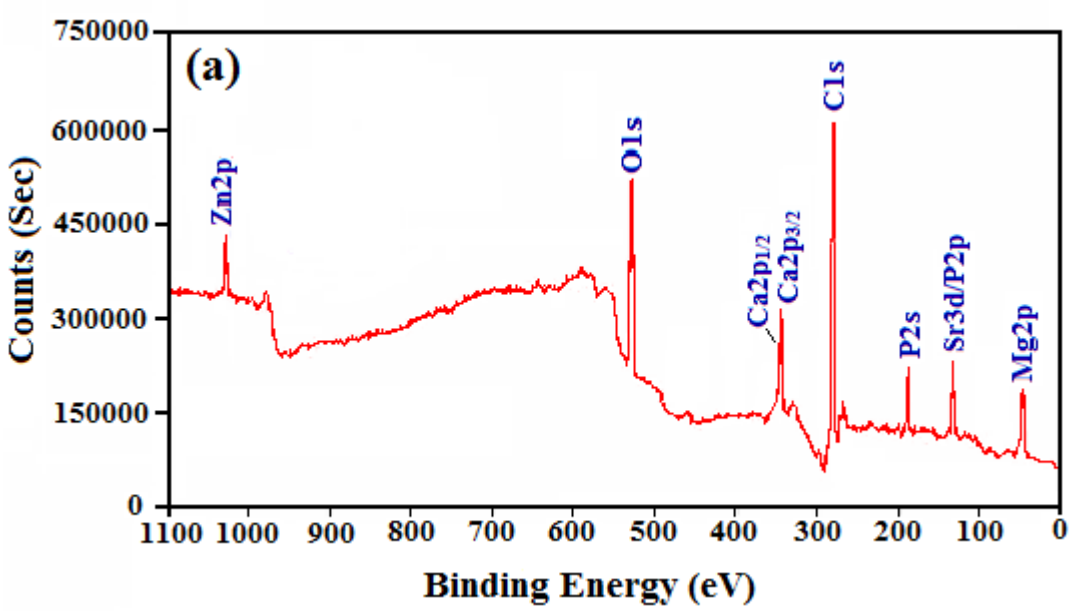

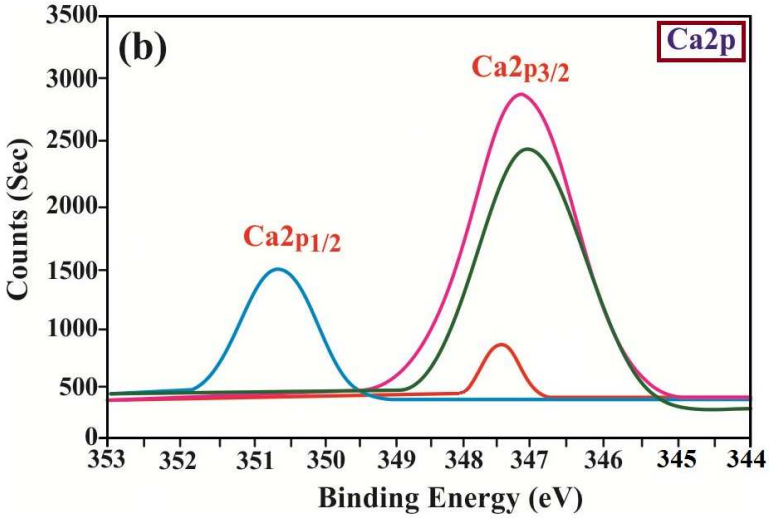

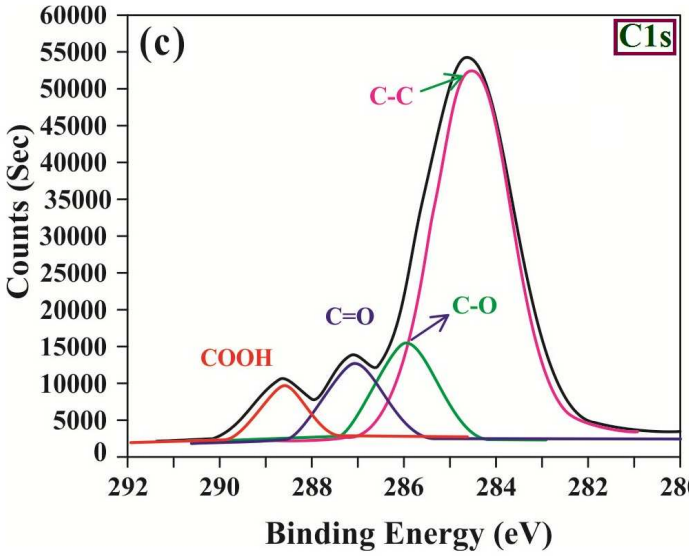

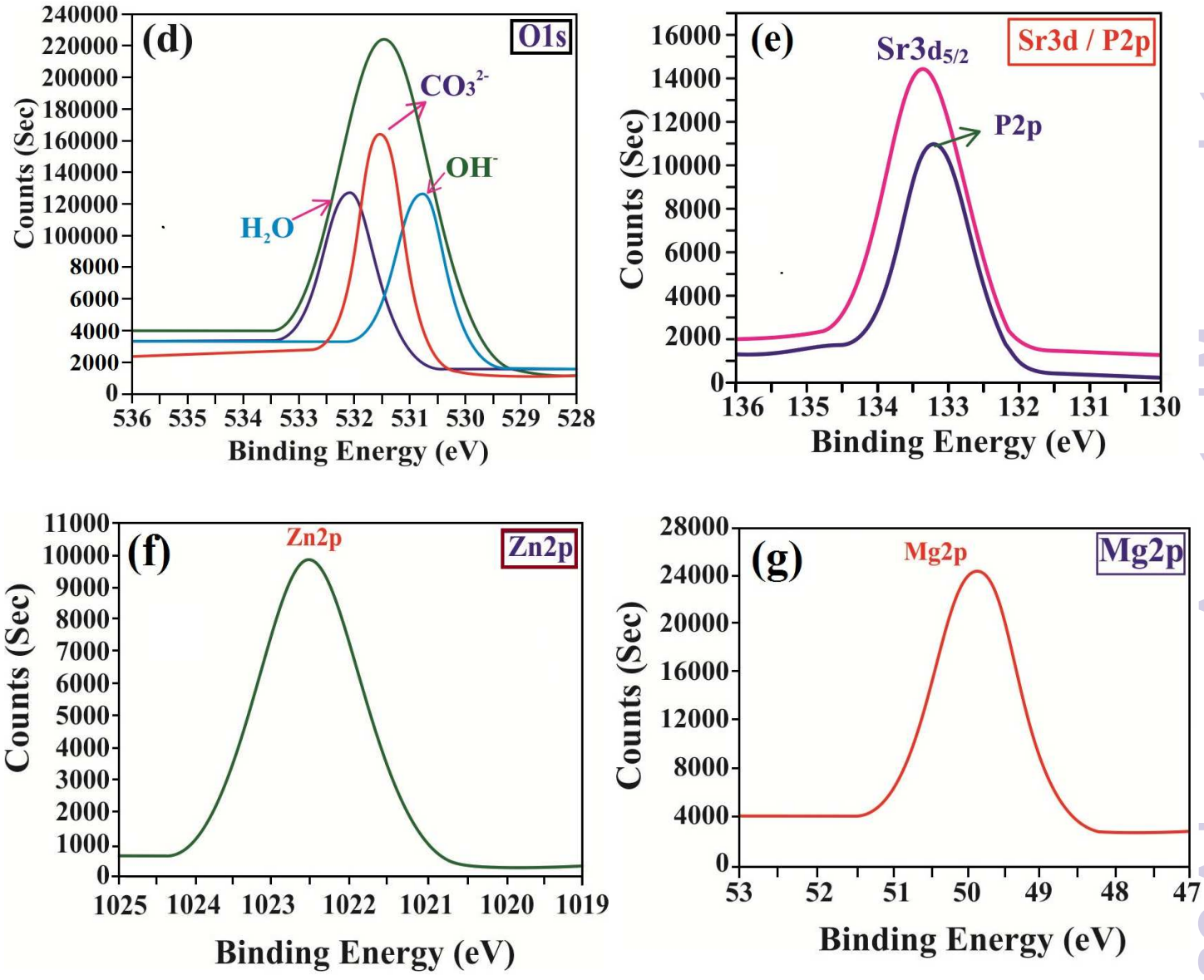

Fig. 6 XPS analysis of the CNT/M-HAP composite coating (a) survey scanning of the CNT/M-HAP composite, and deconvolution spectra of (b) Ca2p, (c) C1s, (d) O1s, (e) Sr3d/P2p, (f) Zn2p and (g) Mg2p for the CNT/M-HAP composite coating.

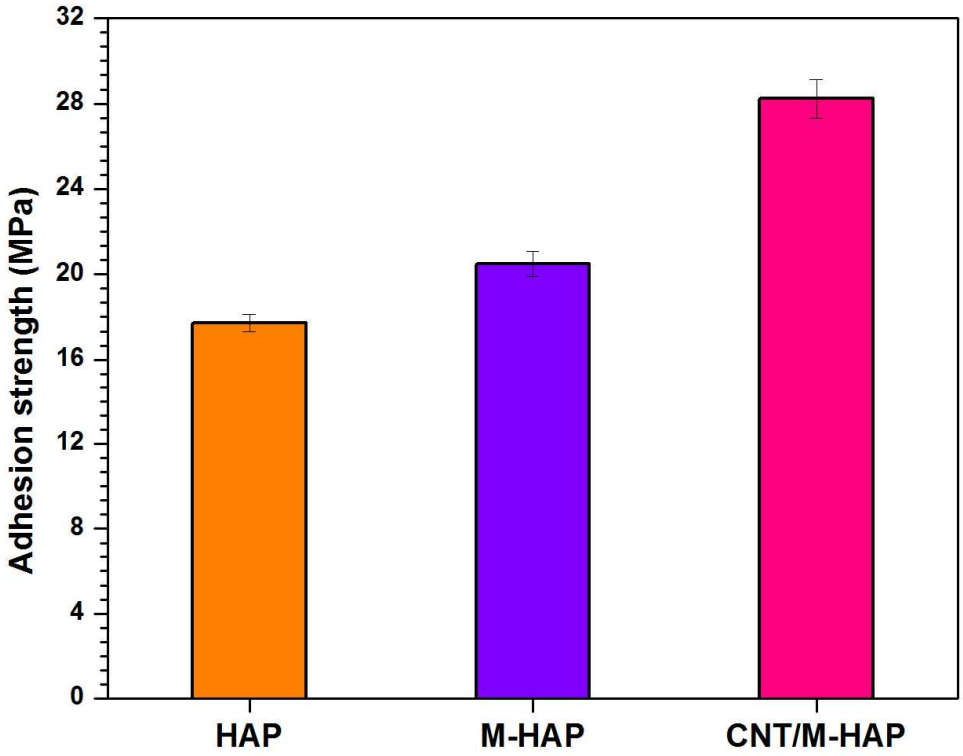

Fig. 7 Adhesion strength of HAP, M-HAP and CNT/M-HAP composite coatings on Ti.

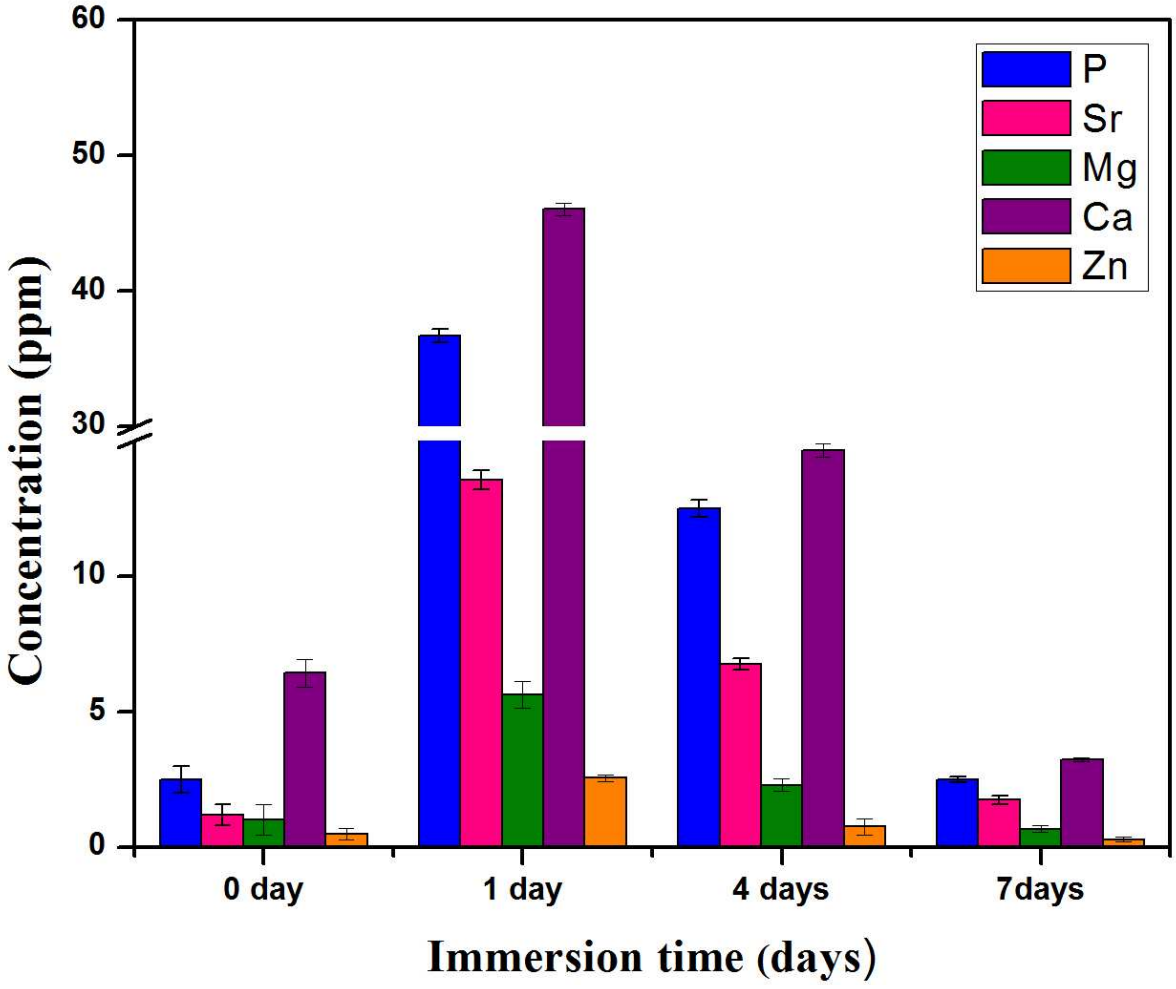

Fig. 8 ICP-AES analysis of CNT/M-HAP composite coating on Ti at different days of immersion.

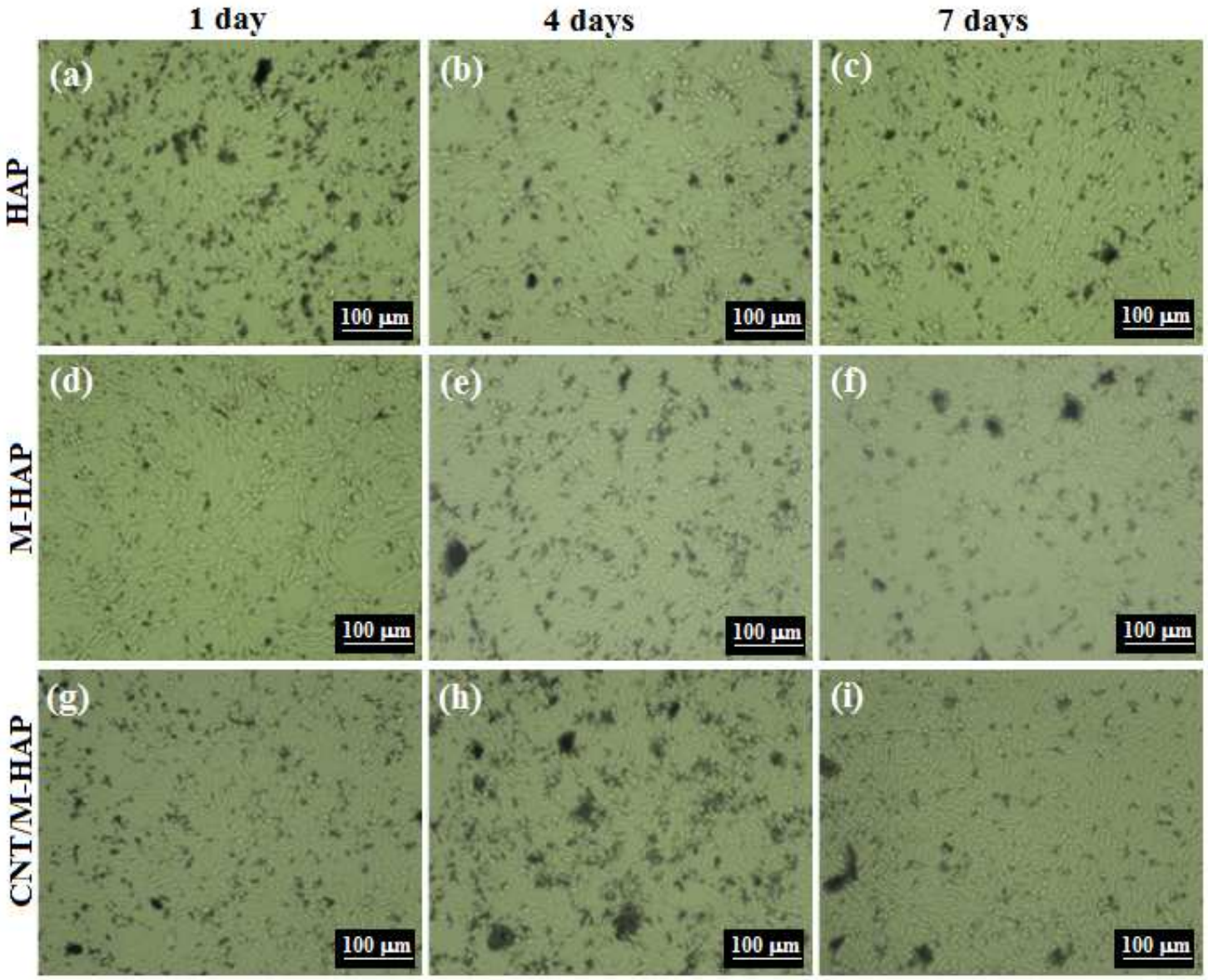

Fig. 9 Optical microscopic images of (a,b,c) HAP, (d,e,f) M-HAP and (g,h,i) CNT/M-HAP composite coatings at 1, 4 and 7 days of incubation.

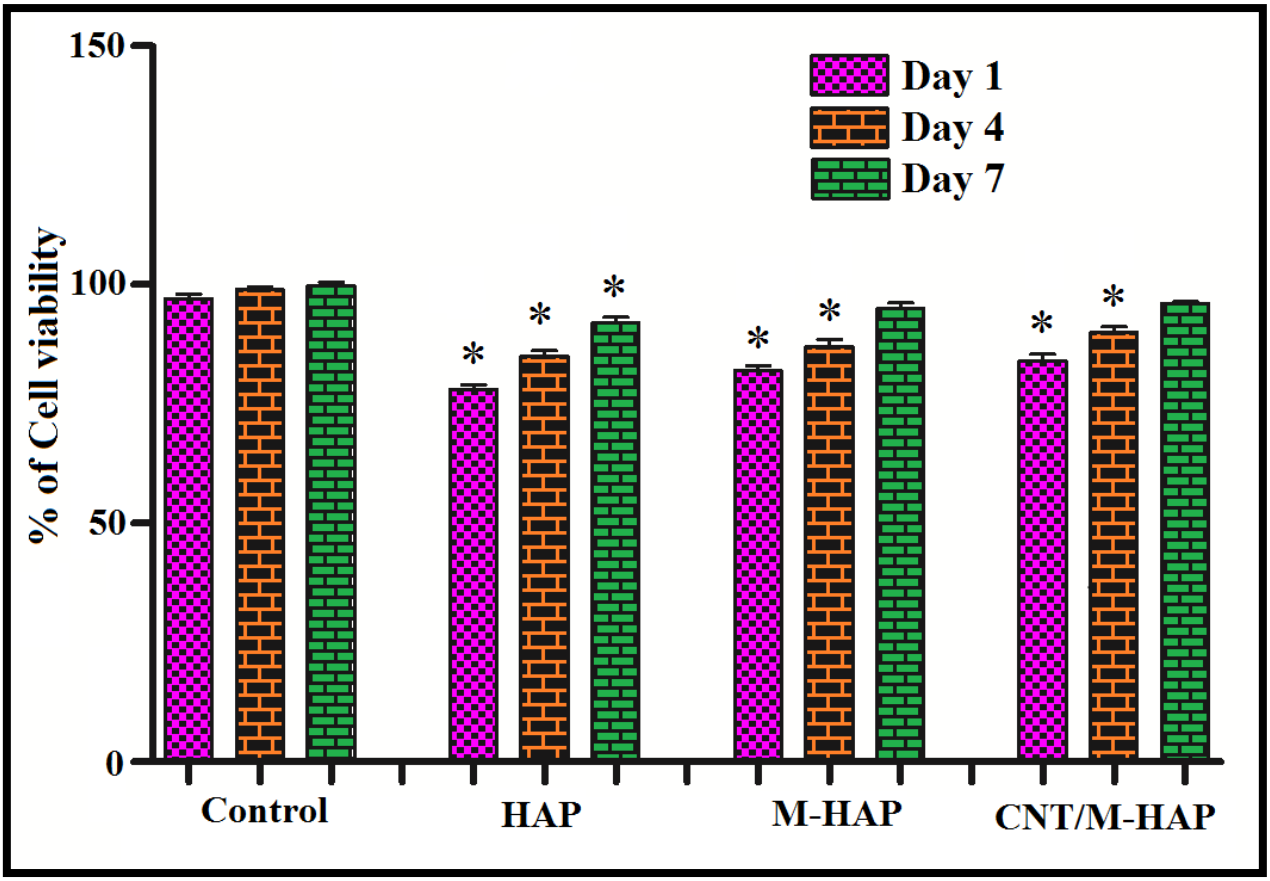

Fig. 10 *In vitro* cytotoxicity results of HAP, M-HAP and CNT/M-HAP coatings on HOS MG63 cells for 1, 4 and 7 days. The asterisk (*) denotes a significant difference compared to control ($P < 0.05$).

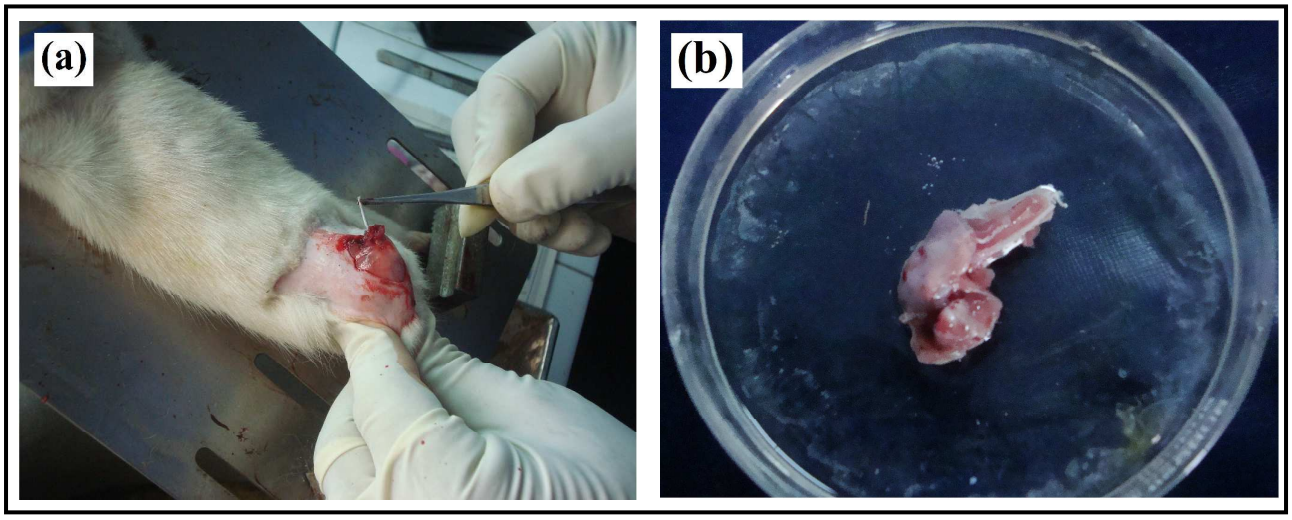

Fig. 11 (a) Ti rod is completely introduced inside the Wistar rat femoral bone. (b) Rat femoral bone retrieved from group 4: CNT/M-HAP composite coated titanium implant at the distal femoral part.

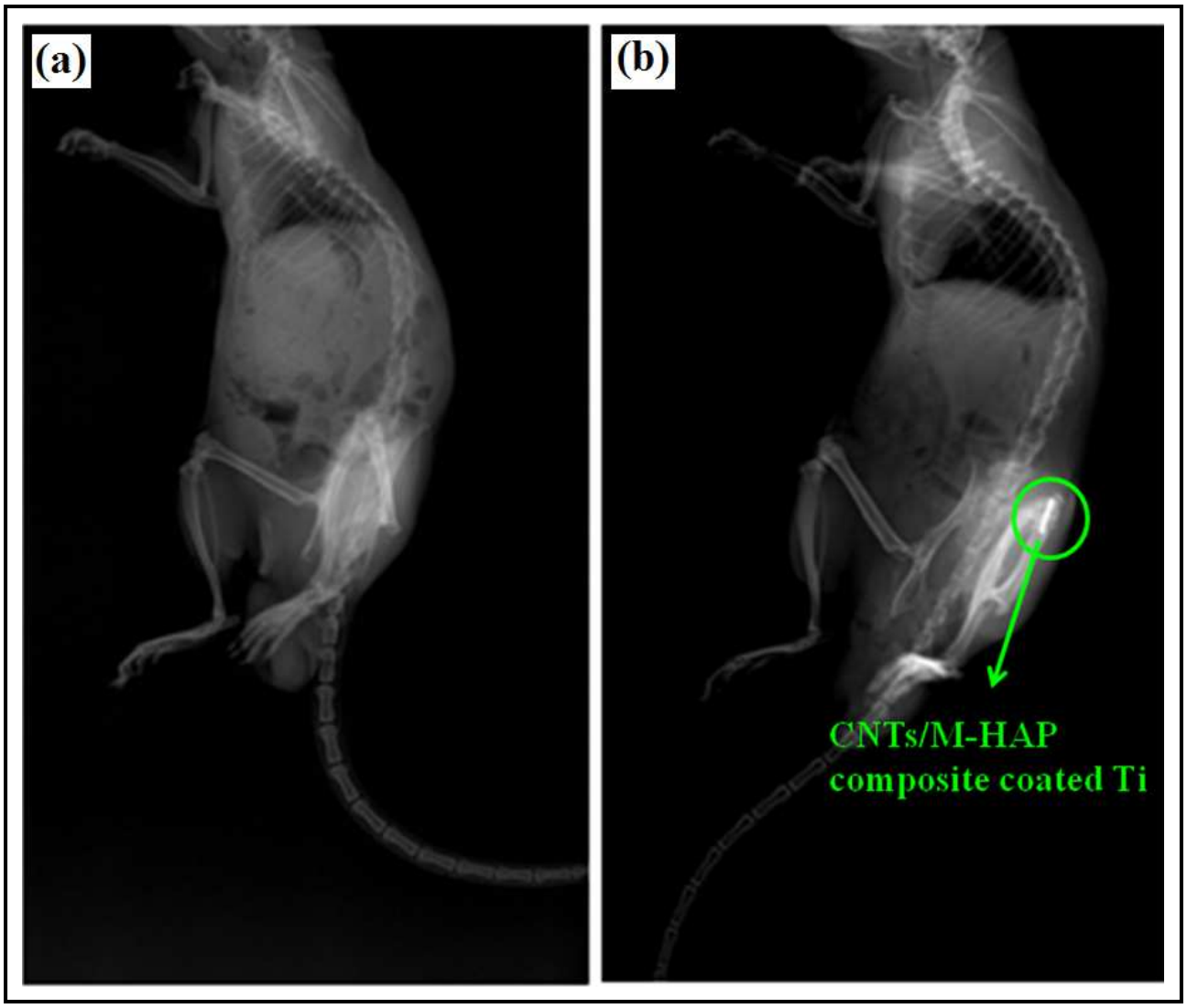

Fig. 12 X-ray photographs of (a) normal rat and (b) implanted rat.

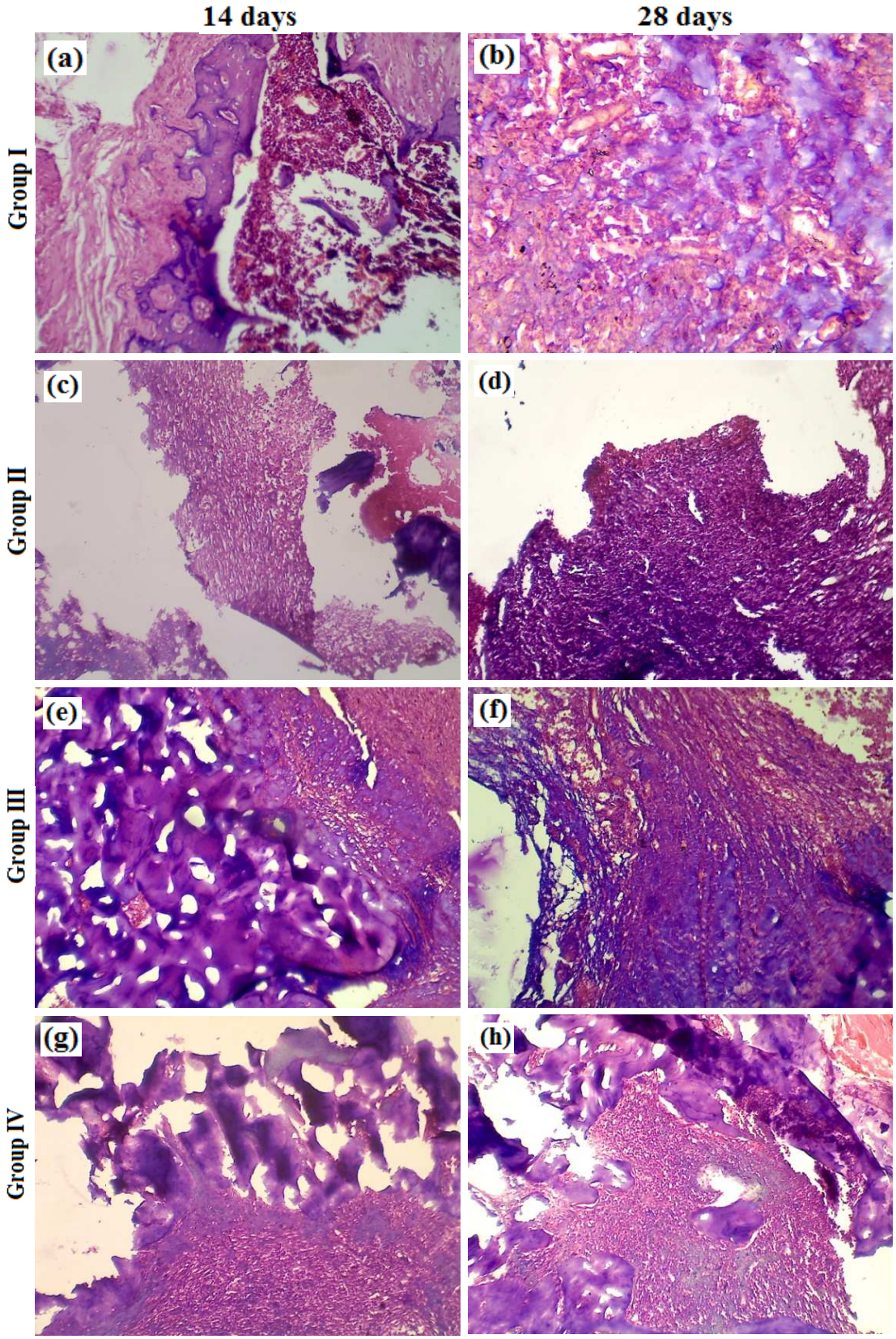

Fig. 13 Toulidene blue stained sections from the group I (a,b), group II (c,d), group III (e,f), group IV (g,h) taken after 14 and 28 days of implantation.

Table 1 Binding energy and atomic percentage of characteristic peaks of XPS spectra of CNT/M-HAP composite coating

S.No.	Core level	Binding Energy	Atomic %
1.	$Ca2p_{3/2}$	347.2	2.253
2.	$Ca2p_{1/2}$	350.7	--
3.	P2p	133.3	0.845
4.	O1s	531.6	37.286
5.	C1s	284.3	45.993
6.	Sr3d	133.4	0.454
7.	Mg2p	49.9	11.623
8.	$Zn2p_{3/2}$	1022.5	1.537